

## A PSO Tuned Fractional-Order PID Controlled Non-inverting Buck-Boost Converter for a Wave/UC Energy System

Erdinc Sahin\*<sup>1</sup>, Ismail H. Altas<sup>2</sup>

Accepted 3rd September 2016

**Abstract:** In this study, a fractional order PID (FOPID) controller is designed and used to control a DC-DC non-inverting buck-boost converter (NIBBC) for a wave/ultra-capacitor (UC) energy system. Because of the energy discontinuities encountered in wave energy conversion systems (WECS), an UC is integrated to the WECS. In order to obtain the best controller performance, particle swarm optimization (PSO) is employed to find the optimum controller parameters. Integral of time weighted absolute error (ITAE) criteria is used as an objective function. Also, an optimized PID controller is designed to test the performance of the FOPID controller. The whole system is developed in Matlab/Simulink/SimPower environment. The simulation results show that the FOPID controller provides lower value performance indices than the PID controller in terms of reducing the output voltage sags and swells.

**Keywords:** Wave energy, Ultra-capacitor, Non-inverting buck-boost converter, Fractional order PID controller, Particle swarm optimization.

### 1. Introduction

Alternative energy sources such as renewable energy are highly considered in order to meet increasing energy demands all over the globe. Among the renewable energy sources, wave energy (WE) is a promising energy source. Its energy density is more available than either solar and wind energy [1]. Whereas, it has some design challenges because of the irregular sea or ocean wave characteristics and extreme weather conditions [2].

A wave energy converter (WEC) used for harvesting energy from the waves. It basically includes a turbine and a floating buoy moves up and down on the sea surface. The power production rate of a WEC is mostly depending on both of the wave height and frequency in a direct-driven WEC. So, the amplitude and frequency of the WEC output voltage fluctuates chaotically. Due to the output power of the WEC has a wide variations, it cannot directly connected to a load or grid. To overcome this problem, WECs are integrated with power electronic devices and storage units [3].

An ultra-capacitor (UC) is an electrochemical capacitor with high-capacitance value. Compared to batteries, it has very long life cycle, high efficiency, high power density and fast charging-discharging capacity [4]. Integration of the UC to WEC with and without power electronic devices can be found in literature [5, 6, 7]. UCs can be directly connected in parallel with an energy source, especially low voltage applications [8]. Also, direct integration of an UC to energy the system increases the overall system efficiency by eliminating the converter losses.

Fractional calculus has become highly popular in engineering applications, especially in control systems. One of the fractional order control method is the fractional order PID controller which is the extension of the PID controller and proposed by Podlubny in 1999 [9]. A FOPID consist of 5 parameters: the proportional gain ( $K_P$ ), integral gain ( $K_I$ ), order of integral ( $\lambda$ ), derivative gain ( $K_D$ ) and order of derivative ( $\mu$ ). These additional two parameters ( $\lambda$ ,  $\mu$ ) increases the complexity of the controller and these parameters should be optimized in order to obtain the best controller performance.

One of the tuning method of controller parameters is to use meta-heuristic algorithms with error-based objective functions. One of these algorithms is the PSO algorithm. PSO is developed by Kennedy and Eberhart in 1995 [10]. The algorithm is an iterative optimization method based on the stochastic movements of the swarms such as fishes and birds and it is suitable for global optimization problems.

In this study, irregular wave effects seen on generated power in a direct-drive WEC are regulated by using an UC energy storage unit and DC-DC NIBB converter in order to obtain a reliable and sustainable load voltage. The parallel connected UC to the WEC provides energy to the load in case of the WEC output is insufficient to supply energy to the load. The converter is controlled by both of FOPID and PID controllers for comparison. PSO algorithm is used to tune the parameters of the both controllers by minimizing the ITAE performance index. The system results with and without UC connection are also discussed.

This paper is organized as follows. Wave energy conversion system with the subtiles wave energy converter, NIBB converter and UC modelling are presented in Section 2. FOPID controller is described in Section 3. PSO algorithm is given in Section 4. In Section 5, the simulation results are discussed. Finally, conclusion is stated in Section VI.

<sup>1</sup> Sürmene Abdullah Kanca VHS, Karadeniz Technical University, 61530-Trabzon, Turkey.

<sup>2</sup> Department of Electrical and Electronics Engineering, Karadeniz Technical University, 61080-Trabzon, Turkey.

\* Corresponding Author: Email: esahin@ktu.edu.tr

Note: This paper has been presented at the 3<sup>rd</sup> International Conference on Advanced Technology & Sciences (ICAT'16) held in Konya (Turkey), September 01-03, 2016.

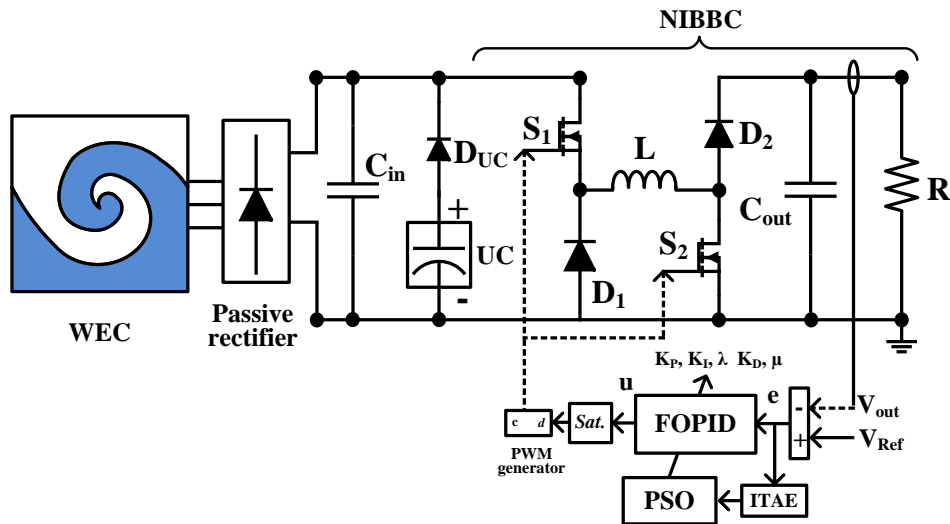


Figure 1. Schematic of the designed WEC.

## 2. Wave Energy Conversion System

The scheme of the whole system is depicted in (Figure.1). The proposed system includes wave energy converter (WEC), 3-phase passive rectifier used for translating produced three phase AC voltage signal from waves to DC signal, UC energy storage unit, NIBB converter and the resistive load.

The aforementioned subsystems are described below, respectively.

### 2.1. Mathematical Model of the Wave Energy Converter

A permanent magnet linear generator (PMLG) is modelled in this study for simulating the electrical energy dynamics of a WEC [11]. The mathematical description of the induced 3-phase voltages with 120o phase shifts are given below.

$$V_A = -\frac{2\pi N\phi_0}{\lambda} \cos\left(\frac{2\pi}{\lambda}x\right) \frac{dx}{dt} \quad (1)$$

$$V_B = -\frac{2\pi N\phi_0}{\lambda} \cos\left(\frac{2\pi}{\lambda}x + \frac{2\pi}{3}\right) \frac{dx}{dt} \quad (2)$$

$$V_C = -\frac{2\pi N\phi_0}{\lambda} \cos\left(\frac{2\pi}{\lambda}x - \frac{2\pi}{3}\right) \frac{dx}{dt} \quad (3)$$

where  $x$  is the translator displacement,  $\lambda$  is the wave length,  $\Phi_0$  is the induced flux magnitude and  $N$  is the number of coil turns.

### 2.2. Non-inverting Buck-Boost Converter

A NIBBC is a type of switched mode DC-DC converter which is used as an interfacing circuit between the wave/UC energy system and the resistive load in this study. Output voltage of the converter which has the same polarity with the input voltage can be lower or higher than magnitude of the input voltage. This means that the converter is able to operate either a buck or boost converter. The proposed converter topology provides a wide input voltage range with low component stress and simplicity [12].

The converter topology pointed out in (Figure.1) consists of an inductor ( $L$ ), diodes ( $D_1, D_2$ ), switching mosfet ( $S_1, S_2$ ) and output capacitor filter ( $C_{out}$ ). The converter parameters and design criteria are given in Table 1.

Using Kirchoff's voltage and current laws, dynamics of the converter is described by (Equations.4 to 5).

$$L \frac{di_L(t)}{dt} = (u-1)V_{out}(t) + uV_{in}(t) \quad (4)$$

$$C \frac{dV_{out}(t)}{dt} = (1-u)i_L(t) - \frac{V_{out}(t)}{R} \quad (5)$$

where  $i_L$  is the inductor current,  $V_{out}$  is the output voltage,  $u$  is the control signal representing the switches positions. ( $u=1$  means the switches are on and  $u=0$  means the switches are off) [12].

When both of the switches are ON-state, as shown in (Figure.2), both of the diodes are reverse biased. Current coming from the source flows through the inductor and so, the inductor is linearly charged. The load voltage is provided by the capacitor.

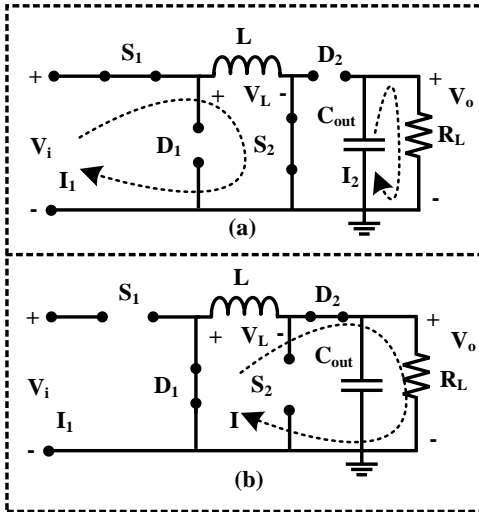
When the switches are OFF-state, the diodes are forward biased and the charged inductor supplies energy to the load and capacitor.

Table 1. NIBBC design parameters.

Parameters	Units	Values
Sampling time	$\mu s$	20
Switching frequency	kHz	5
Desired output voltage	V	12
Input capacitor	$\mu F$	13400
Output capacitor	$\mu F$	9800
Inductor	mH	0.44
Diodes forward voltages	V	0.8
Load resistor	$\Omega$	10

### 2.3. Ultra-capacitor Modelling

Different type of model topologies of UC can be found in literature. Some of these are R-C parallel branch model [13], R-C transmission line model [14] and R-C classical model [13, 15], etc.



**Figure 2.** Operational modes of the NIBBC. (a) Switches are ON-state, (b) Switches are OFF-state.

R and C are used to symbolize resistor and capacitor of the UC, respectively. In this study, RC classical model is used to simulate UC electrical dynamics. The classical R-C topology is suitable for slow discharging applications and pulse loads. Also, it is easy to model [16]. The proposed model equivalent circuit is shown below.

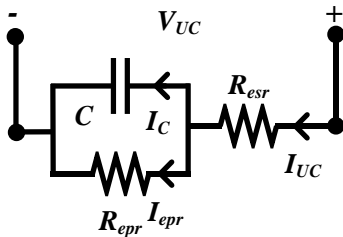


**Figure 3.** Equivalent circuit of the R-C modelled UC.

where  $V_{UC}$  is the terminal voltage of the UC,  $I_{UC}$  is the current flowing through UC,  $R_{esr}$  is the equivalent series resistance used to simulate internal resistance of the UC,  $R_{epr}$  is the equivalent parallel resistance used to simulate leakage currents and  $C$  is the capacitance of the UC. The mathematical description between the UC voltage and current are given by (Equation.6).

$$V_{UC(final)}(t) = I_{UC}(t)R_{esr} + \frac{1}{C} \int_0^t I_C(t)dt + V_{UC(initial)}(t) \quad (6)$$

Maxwell BMOD0083-P048 ultra-capacitor specifications are used for modelling of the UC in this study. The parameters of the UC are listed in Table 2 [17].

**Table 2.** Ultra-capacitor specifications.

Parameters	Units	Values
Rated capacitance (C)	F	83
Equivalent series resistance (ESR)	mΩ	10
Rated voltage	V	48
Power density	W/kg	2700
Maximum energy density	Wh/kg	2.6

### 3. Fractional Order PID Controller

Fractional-order PID controller based on fractional calculus includes more than two additional parameters ( $\lambda, \mu$ ) compared to conventional PID controller.  $\lambda$  is the order of the integrator and  $\mu$  is the order of differentiator. These two additional parameters provides design flexibility and robustness to the controller. However, optimal parameter tuning of the controller becomes more complex because of the increased controller parameters.

Riemann-Liouville (RL) derivative definition is one the well-known definitions used for fractional calculus and its fractional definition of order  $\alpha$  of function  $f(t)$  is given by (Equation.7) [9].

$${}_r D_t^\alpha f(t) = \frac{1}{\Gamma(n-\alpha)} \frac{d^n}{dt^n} \int_r^t \frac{f(\tau)}{(t-\tau)^{\alpha-n+1}} d\tau \quad (7)$$

where  $n$  is an integer,  $n-1 < \alpha < n$  and  $\Gamma(z)$  is the Gamma function. The FOPID controller has five parameters to be optimized in order to obtain the best controller performance. The block diagram representation of the proposed controller is shown in (Figure.4).

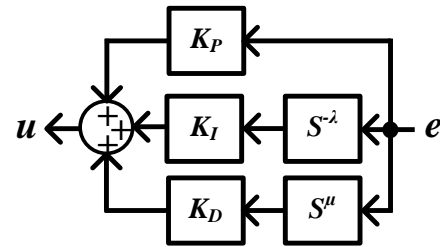


**Figure 4.** Block diagram of the FOPID controller.

A FOPID controller transfer function representation is defined as [18]:

$$G_{FOPID}(s) = \frac{U(s)}{E(s)} = \left( K_P + \frac{K_I}{s^\lambda} + K_D s^\mu \right) \quad (8)$$

where  $U(s)$  and  $E(s)$  are the control and error signals, respectively. In this study, FOPID controller software are performed by FOMCON Toolbox [19].

### 4. Particle Swarm Optimization

Particle swarm optimization (PSO) is a population based evolutionary algorithm developed from the simulations of bird-flocking. The first step in algorithm is that the specified number of particles are placed randomly in the  $d$ -dimensional search space and objective function of the each particle is calculated and saved at their current position [10].

Associated coordinates with the best solution is called  $p_{best}$ . Then, the obtained best solution is compared to each other to find the global best solution which is called as  $g_{best}$ . The movements of the particles are updated by using the position ( $X$ ) and velocity ( $V$ ) functions given in (Equation.9 to 10), respectively [20].

$$V_i^{t+1} = wV_i^t + c_1 r_1 (p_{best}^t - X_i^t) + c_2 r_2 (g_{best}^t - X_i^t) \quad (9)$$

$$X_i^{t+1} = X_i^t + V_i^{t+1} \quad (10)$$

In (9) and (10),  $i$  is the particle number,  $t$  is the iteration number,  $c_1$  and  $c_2$  are the acceleration factors which are set to 2.  $r_1$  and  $r_2$  are the random numbers in the range of [0, 1].  $w$  is the inertia weight which balances the global and local search. The value of the  $w$  is linearly decreased from 0.9 to 0.4 as recommended in

[21]. Population size ( $n$ ) and the iteration number ( $N$ ) for both of the controller tuning processes are set to 10 and 20, respectively. Since ITAE criteria of which mathematical description given below provides a smaller overshoot and reduced oscillations than the other error-based performance indexes, it is used as an objective function [22, 23].

$$ITAE = \int_0^t |e(t)| dt \quad (11)$$

## 5. Simulation Results

The WECS illustrated schematically in (Figure.1) is developed in Matlab/Simulink/SimPower environment. Because the small-scale waves are considered in this study, current drawing from the generator is limited by duty cycle ( $d$ ) in the range of [0, 0.65]. Simulations are performed for 30 seconds. The initial charge voltage of the UC is 12 V and the load resistor is 10  $\Omega$ .

The DC-DC NIBB converter used for load voltage regulation is controlled by both of FOPID and classical PID controllers. PSO algorithm is employed to tune controller parameters and ITAE performance measure is used as an objective function. Also, other error-based performance indexes : integral of squared error (ISE), integral of absolute error (IAE) and integral of time weighted squared error (ITSE) are considered for a better comparison of the designed controllers. The optimized parameters of the controllers and calculated performance measures are given in Table 3 and Table 4, respectively.

**Table 3.** Optimized controller parameters.

Controller type	Controller parameters				
	$K_P$	$K_I$	$\lambda$	$K_D$	$\mu$
FOPID	13.42	27.78	1.41	0.0153	0.34
PID	12.11	29.78	-	0.0794	-

**Table 4.** Performance measures.

Controller type	Performance results			
	ITAE	IAE	ITSE	ISE
FOPID	51.39	3.535	7.129	1.287
PID	61.10	4.196	10.77	1.659

The simulation results are considered with and without UC unit. Since the FOPID controller provides lower value performance criteria value, all results are shown with optimized FOPID controller.

The induced irregular 3-phase form in WEC with and without UC unit is depicted in (Figure.5). The converter input voltage and current is shown in (Figure.6).

(Figure.6) shows that the parallel connected UC unit to the WEC output eliminates the voltage drops encountered in the WEC because of the irregular wave effects. As a result, a more stable input voltage is obtained for the NIBBC input. WEC provides energy to the load when the induced voltage value is greater than UC charge voltage.

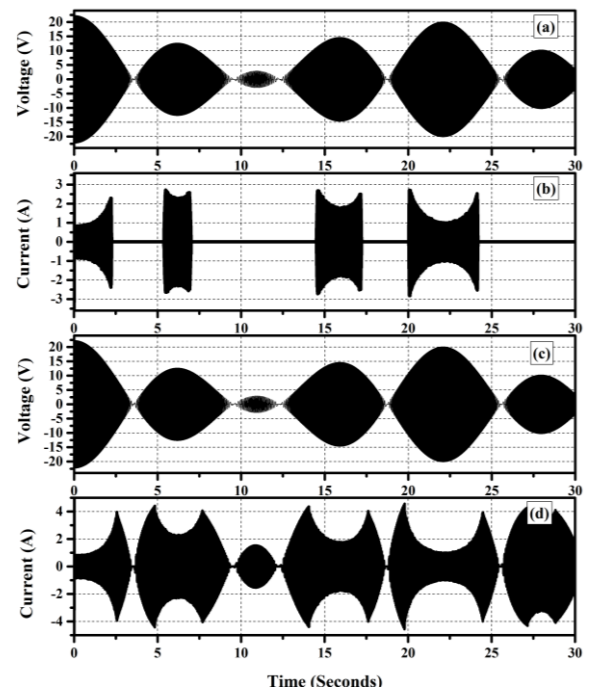


**Figure 5.** WEC phase to phase voltage and phase currents with (a, b) and without (c, d) UC unit.

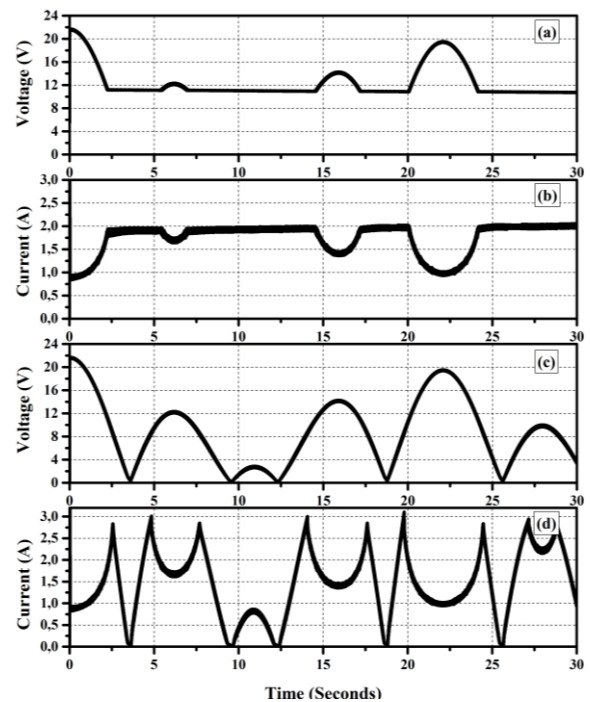


**Figure 6.** DC-DC NIBB converter input voltage and current with (a, b) and without (c, d) UC unit.

(Figure.7) shows the load voltage and current with and without UC bank. The WEC is alone inefficient to meet the load power requirement. The comparison of the PSO optimized FOPID and PID controllers are given in (Figure.8). The FOPID controller provides a stable voltage with increased quality than the PID controller. Also, the system response without overshoot is obtained by FOPID controller.

## 6. Conclusion

In this study, an initially charged UC unit is connected in parallel with a WEC output. A NIBBC is used as an interface circuit between the WEC/UC side and the load.

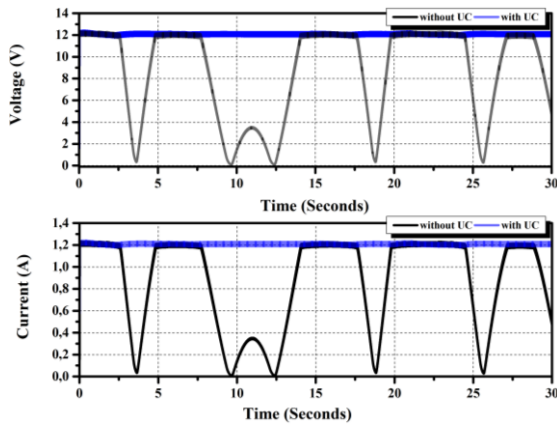


Figure 7. Load voltage and current with and without UC.

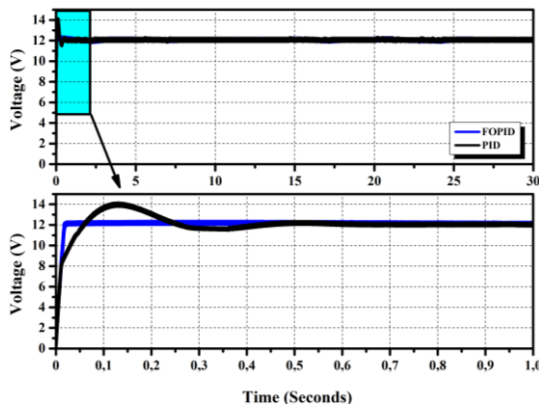


Figure 8. Comparison of the FOPID and PID controlled load voltage with UC.

Thus, it is aimed to regulate the energy irregularities encountered in WEC output.

The designed WECS is tested under irregular wave condition. The rectified variable WEC/UC output voltage is applied to the NIBBC. DC-DC converter is controlled by a FOPID controller. Also, a classical PID controller is used for comparison. In tuning process of the both controller parameters, a well-known optimization algorithm PSO is employed. The ITAE is used as an objective function. The simulation results show that the FOPID provides lower value objective function value than PID controller. This means the higher quality output voltage without overshoot is obtained by using the FOPID controller.

Since the small-scale waves are considered for this study, WEC is alone inefficient to charge the UC unit. A solar or grid charged UC can be considered to increase the overall system sustainability.

## Acknowledgements

This study was supported by Karadeniz Technical University Scientific Research Projects Unit. Project No: FBA-2014-5168.

## References

[1] Muetze, A., and Vining, J. G. (2006). Ocean wave energy conversion-a survey. IEEE Industry Applications Conference Forty-First IAS Annual Meeting. Vol. 3. Pages. 1410-1417.

[2] Czech, B., and Bauer, P. (2012). Wave energy converter concepts: Design challenges and classification. IEEE Industrial Electronics Magazine. Vol. 6. Pages. 4-16.

[3] Hong, Y., Waters, R., Boström, C., Eriksson, M., Engström, J., and Leijon, M. (2014). Review on electrical control

strategies for wave energy converting systems. Renewable and Sustainable Energy Reviews. Vol. 31. Pages. 329-342.

[4] Conway, B. E. (2013). Electrochemical supercapacitors: scientific fundamentals and technological applications. Springer Science & Business Media.

[5] Hazra, S., and Bhattacharya, S. (2012). Short time power smoothing of a low power wave energy system. 38<sup>th</sup> Annual IEEE Industrial Electronics Conference (IECON). Pages. 5846-5851.

[6] Murray, D. B., Hayes, J. G., O'Sullivan, D. L., and Egan, M. G. (2012). Supercapacitor testing for power smoothing in a variable speed offshore wave energy converter. IEEE Journal of Oceanic Engineering. Vol. 37. Pages. 301-308.

[7] Kovaltchouk, T., Multon, B., Ahmed, H. B., Aubry, J., and Venet, P. (2015). Enhanced aging model for supercapacitors taking into account power cycling: Application to the sizing of an Energy Storage System in a Direct Wave Energy Converter. IEEE Transactions on Industry Applications. Vol. 51. Pages. 2405-2414.

[8] Uzunoglu, M., and Alam, M. S. (2006). Dynamic modeling, design, and simulation of a combined PEM fuel cell and ultracapacitor system for stand-alone residential applications. IEEE Transactions on Energy Conversion. Vol. 21. Pages. 767-775.

[9] I. Podlubny. (1999). Fractional Differential Equations, Academic Press, San Diego.

[10] Eberhart, R. C., and Kennedy, J. (1995). A new optimizer using particle swarm theory. In Proceedings of the sixth international symposium on micro machine and human science. Vol. 1. Pages. 39-43.

[11] Hong, Y., Eriksson, M., Castellucci, V., Boström, C., and Waters, R. (2016). Linear generator-based wave energy converter model with experimental verification and three loading strategies. IET Renewable Power Generation. Vol. 10. Pages. 349-359.

[12] H. Sira-Ramirez, and R. Silva-Ortigoza. (2006). Control design techniques in power electronic devices. Springer Science and Business Media.

[13] L. Zubietta, and R. Boner. (2000). Characterization of double-layer capacitors for power electronics applications. IEEE Transactions on Industrial Applications Vol. 36. Pages. 199-205.

[14] De Levie, R. (1963). On porous electrodes in electrolyte solutions: I. Capacitance effects. Electrochimica Acta. Vol. 8. Pages. 751-780.

[15] Spyker, R. L., & Nelms, R. M. (2000). Classical equivalent circuit parameters for a double-layer capacitor. IEEE Transactions on Aerospace and Electronic Systems. Vol. 36. Pages. 829-836.

[16] Nelms, R. M., Cahela, D. R., and Tatarchuk, B. J. (2003). Modeling double-layer capacitor behavior using ladder circuits. IEEE Transactions on Aerospace and Electronic Systems. Vol. 39. Pages. 430-438.

[17] Maxwell Technologies. BMOD0083-P048 ultracapacitor datasheet. [Online]. Available: www.maxwell.com.

[18] I. Podlubny. (1999). Fractional-order systems and PI<sup>λ</sup>D<sup>μ</sup> controllers. Transactions Automation Control. Vol. 44. Pages. 208-213.

[19] Tepljakov, A., Petlenkov, E., and Belikov, J. (2011). FOMCON: Fractional-order modeling and control toolbox for MATLAB. 18<sup>th</sup> International Mixed Design of

Integrated Circuits and Systems (MIXDES) Conference. Pages. 684-689.

- [20] R. Poli, J. Kennedy, T. Blackwell. (2007). Particle swarm optimization. *Swarm Intelligence*. Vol. 1. Pages. 33–57.
- [21] Gaing, Z. L. (2004). A particle swarm optimization approach for optimum design of PID controller in AVR system. *IEEE transactions on energy conversion*. Vol. 19. Pages. 384-391.
- [22] Schultz, W. C., and Rideout, V. C. (1961). Control system performance measures: Past, present, and future. *IRE Transactions on Automatic Control*. Vol. 1. Pages. 22-35.
- [23] Nagrath, I. J. (2006). *Control systems engineering*. New Age International.